Production of three isolated photons in the parton Reggeization approach at high energies

A. V. Karpishkov[*] and V. A. Saleev[†]

Samara National Research University, Moskovskoe Shosse, 34, 443086 Samara, Russia and Joint Institute for Nuclear Research, Dubna 141980, Russia

(Received 27 May 2022; accepted 6 September 2022; published 29 September 2022)

We study a large-p_T three-photon production in the proton-proton collisions at the LHC. We use the leading order (LO) approximation of the parton Reggeization approach consistently merged with the next-to-leading order corrections originating from the emission of the additional jet. For numerical calculations, we apply the parton-level generator KaTie and the modified Kimder-Martin-Ryskin-type unintegrated parton distribution functions, which satisfy the exact normalization conditions for arbitrary x. We compare our prediction with data from the ATLAS collaboration at the center-of-mass energy $\sqrt{s} = 8$ TeV. We find that the inclusion of the real next-to-leading-order corrections leads to a good agreement between our predictions and data with the same accuracy as for the next-to-next-to-leading calculations based on the collinear parton model of QCD. At higher energies ($\sqrt{s} = 13$ and 27 TeV) the parton Reggeization approach predicts larger cross sections, up to ∼15% and ∼30%, respectively.

DOI: 10.1103/PhysRevD.106.054036

I. INTRODUCTION

The recent experimental data for a large-p_T multiphoton production at the Tevatron [1,2] and the LHC [3–5] at the energy range from 1.96 TeV up to 8 TeV are extensively studied in the collinear parton model (CPM) of perturbative quantum chromodynamics (QCD) beyond the leading-order (LO) accuracy in strong-coupling constant, α_S, i.e., at the next-to-leading-order (NLO) [6–8] and even at the next-to-next-to-leading-order (NNLO) [9–12]. The high-order calculations for the two-photon or the three-photon production in CPM of QCD provides rather bad agreement with the data at a level of the NLO accuracy. For example, NLO QCD calculations strongly underestimate, by a factor of 2 or even more, recent data from ATLAS Collaboration at $\sqrt{s} = 8$ TeV [5] for the three-photon production. The inclusion of additional contributions from the parton-shower mechanism and hadronization effects [7] to the NLO calculations increase theoretical prediction but they are yet far from the measured cross sections.

Inclusion of the NNLO QCD corrections for the two-photon production [9] and the three-photon production [11,12] eliminates the existing discrepancy with respect to the NLO QCD predictions. However, for three-photon production, the agreement with data is not so good as for two-photon production. Moreover, it is achieved only the hard scale parameter μ should very small relatively usual used value [11].

In the CPM of QCD, we neglect the transverse momenta of initial-state partons in hard-scattering amplitudes is a correct assumption for the fully inclusive observables, such as p_T-spectra of single prompt photons or jets, where their large transverse momentum defines a single hard scale of the process, $\mu \sim p_T$. The corrections breaking the collinear factorization are shown to be suppressed by powers of the hard scale [13].

The multiphoton large-p_T production is a multiscale hard process in which using the simple collinear picture of the initial state radiation may be a bad approximation. In the present paper, we calculate the different multiscale variables in three-photon production in a framework of the high-energy factorization (HEF) or the k_T-factorization, which initially has been introduced as a resummation tool for $\ln(\sqrt{s}/\mu)$-enhanced corrections to the hard-scattering coefficients in CPM, where invariants $\sqrt{s}$ referees to the total energy of the process. We use the parton Reggeization approach (PRA), which is a version of the HEF formalism, based on the modified multi-Regge kinematics (mMRK) approximation for the QCD scattering amplitudes. This approximation is accurate both in the collinear limit, which drives the transverse-momentum-dependent (TMD) factorization [13] and in the high-energy (Mmulti-Regge) limit, which is important for Balitsky-Fadin-Kuraev-Lipatov

[*]karpishkoff@gmail.com
[†]saleev@samsu.ru

(BFKL) [14–17] resummation of $\ln(\sqrt{s}/\mu)$-enhanced effects.

Working in the PRA, we have studied previously the one-photon production [18], the two-photon production [19], and the photon plus jet production [20] in proton-(anti)proton collisions at the Tevatron and the LHC. In the present paper, we study the production of the three isolated photons at the LHC. Preliminary, our predictions have been presented as a short note at DIS2021 Conference, see Ref. [21]. A similar study of three-photon production in the k_T-factorization approach was published recently in Ref. [22], where authors compared predictions obtained with different unPDFs [23–26] that is the compliment to our study in the PRA [21].

The paper has the following structure, in Sec. II the relevant basics of the PRA formalism are outlined. In the Sec. III we overview Monte-Carlo (MC) parton-level event generator KaTie and the relation between PRA and MC calculations using KaTie for the tree-level amplitudes. In the Sec. IV we compare obtained in the PRA results with the recent ATLAS [5] data as well as with the theoretical predictions obtained in NNLO calculations of the CPM [11,12]. Our conclusions are summarized in the Sec. V.

II. PARTON REGGEIZATION APPROACH

The PRA is based on high-energy factorization for hard processes in the multi-Regge kinematics. The basic ingredients of PRA are k_T-dependent factorization formula, unintegrated parton distribution functions (unPDF's) and gauge-invariant amplitudes with off-shell (Reggeized) initial-state partons. The first one is proved in the leading-logarithmic-approximation of high-energy QCD [27,28], the unPDFs are constructed in the same manner as it was suggested by Kimber, Martin, Ryskin, and Watt [23,24], but with sufficient revision [29]. The off-shell amplitudes are derived using Lipatov's effective field theory (EFT) of Reggeized gluons [30] and Reggeized quarks [31]. The brief description of LO in α_S approximation of PRA is presented below. More details can be found in Refs. [32,33], the inclusion of real NLO corrections in the PRA was studied in Ref. [33], the development of PRA in the full one-loop NLO approximation was further discussed in [34–36].

The factorization formula of the PRA in LO approximation for the arbitrary process $p + p \to \mathcal{Y} + X$, can be obtained from the factorization formula of the CPM for the auxiliary hard subprocess like $g + g \to q + \mathcal{Y} + \bar{q}$. For the discussed here process of three-photon production, $\mathcal{Y} = \gamma\gamma\gamma$. In the Ref. [33] the modified Multi-Regge Kinematics (mMRK) approximation for the auxiliary amplitude has been constructed, which correctly reproduces the multi-Regge and collinear limits of corresponding QCD amplitude. This mMRK-amplitude has t-channel factorized form, which allows one to rewrite the cross section of the auxiliary subprocess in a k_T-factorized form:

$$d\sigma = \sum_{i,\bar{j}} \int_0^1 \frac{dx_1}{x_1} \int \frac{d^2\mathbf{q}_{T1}}{\pi} \tilde{\Phi}_i(x_1, t_1, \mu^2) \int_0^1 \frac{dx_2}{x_2} \times \int \frac{d^2\mathbf{q}_{T2}}{\pi} \tilde{\Phi}_j(x_2, t_2, \mu^2) \cdot d\hat{\sigma}_{\mathrm{PRA}}, \tag{1}$$

where $t_{1,2} = -\mathbf{q}^2_{T1,2}$, the off-shell partonic cross section $\hat{\sigma}_{\mathrm{PRA}}$ in the PRA is determined by squared Reggeized amplitude, $\overline{|\mathcal{A}_{\mathrm{PRA}}|^2}$. Despite the fact that four-momenta $(q_{1,2})$ of partons in the initial state of amplitude $\mathcal{A}_{\mathrm{PRA}}$ are off-shell $(q^2_{1,2} = -t_{1,2} < 0)$, the PRA hard-scattering amplitude is gauge-invariant because the initial-state off-shell partons are treated as Reggeized partons of gauge-invariant EFT for QCD processes in multi-Regge kinematics (MRK), introduced by L.N. Lipatov in [30,31]. The Feynman rules of this EFT are written down in the Refs. [31,37].

The tree-level unPDFs $\tilde{\Phi}_i(x_{1,2}, t_{1,2}, \mu^2)$ in Eq. (1) are equal to the convolution of the collinear PDFs $f_i(x, \mu^2)$ and Dokshitzer-Gribov-Lipatov-Altarelli-Parisi (DGLAP) splitting function $P_{ij}(z)$ with the factor $1/t_{1,2}$,

$$\tilde{\Phi}_i(x, t, \mu) = \frac{\alpha_s(\mu)}{2\pi} \frac{1}{t} \sum_{j=q,\bar{q},g} \int_x^1 dz P_{ij}(z) F_j\left(\frac{x}{z}, \mu_F^2\right), \tag{2}$$

where $F_i(x, \mu_F^2) = x f_j(x, \mu_F^2)$. Here and above we put $\mu_F = \mu_R = \mu$. Consequently, the cross section (1) with such unPDFs contains the collinear divergence at $t_{1,2} \to 0$ and soft divergence at $z_{1,2} \to 1$.

To resolve collinear divergence problem of $\tilde{\Phi}_i(x, t, \mu)$ we require that modified unPDF $\Phi_i(x, t, \mu)$ should be satisfied exact normalization condition:

$$\int_0^{\mu^2} dt \Phi_i(x, t, \mu^2) = F_i(x, \mu^2), \tag{3}$$

which is equivalent to:

$$\Phi_i(x, t, \mu^2) = \frac{d}{dt}[T_i(t, \mu^2, x) F_i(x, t)], \tag{4}$$

where $T_i(t, \mu^2, x)$ is usually referred to as Sudakov form-factor, satisfying the boundary conditions $T_i(t = 0, \mu^2, x) = 0$ and $T_i(t = \mu^2, \mu^2, x) = 1$. Such a way, modified unPDF can be written as follows from Kimder-Martin-Ryskin (KMR) model:

$$\Phi_i(x, t, \mu) = \frac{\alpha_s(\mu)}{2\pi} \frac{T_i(t, \mu^2, x)}{t} \times \sum_{j=q,\bar{q},g} \int_x^1 dz P_{ij}(z) F_j\left(\frac{x}{z}, t\right) \theta(\Delta(t, \mu) - z). \tag{5}$$

Here, we resolved also soft divergence by taking into account the observation that the mMRK expression gives

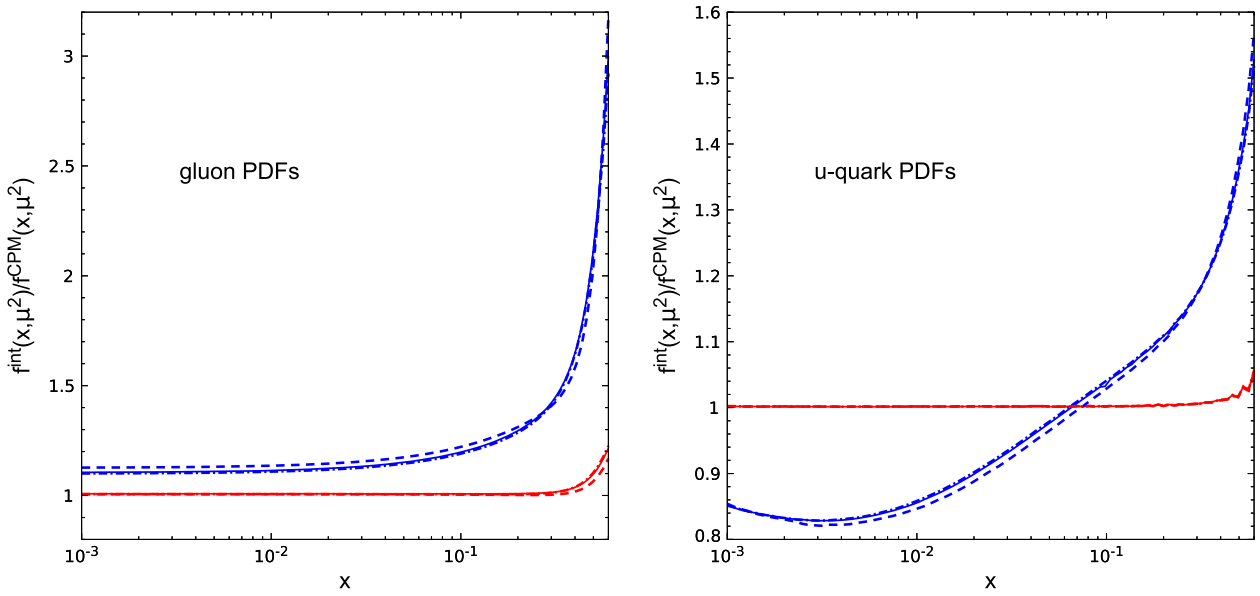

FIG. 1. The ratios of integrated over transverse momentum the gluon (left panel) and the valence u-quark unPDFs to the relevant collinear PDFs as a function of x at the different values of the hard scale $\mu^2 = 10^4, 6\times10^4, 10^5$ GeV^2, which correspond to dashed, solid and dotted-dashed lines. Blue lines are obtained in original KMR model [23,24] and red lines are obtained in our modified model for unPDFs [29].

a reasonable approximation for the exact matrix element only in the rapidity-ordered part of the phase-space. From this requirement, the following cutoff on $z_{1,2}$ can be derived: $z_{1,2} < 1 - \Delta_{\rm KMR}(t_{1,2},\mu^2)$, where $\Delta_{\rm KMR}(t,\mu^2) = \sqrt{t}/(\sqrt{\mu^2}+\sqrt{t})$ is the KMR-cutoff function [23].

The solution for Sudakov form-factor in Eq. (4) has been obtained in Ref. [29]:

$$T_i(t,\mu^2,x) = \exp\left[-\int_t^{\mu^2}\frac{dt'}{t'}\frac{\alpha_s(t')}{2\pi}(\tau_i(t',\mu^2)+\Delta\tau_i(t',\mu^2,x))\right] \tag{6}$$

with

$$\tau_i(t,\mu^2) = \sum_j \int_0^1 dz z P_{ji}(z)\theta(\Delta(t,\mu^2)-z),$$

$$\Delta\tau_i(t,\mu^2,x) = \sum_j \int_0^1 dz\theta(z-\Delta(t,\mu^2)) \times\left[zP_{ji}(z) - \frac{F_j(\frac{x}{z},t)}{F_i(x,t)}P_{ij}(z)\theta(z-x)\right].$$

Let us summarize important differences between the Sudakov form-factor obtained in our mMRK approach (6) and the KMR approach [23]. At first, the Sudakov form-factor (6) contains the x-depended $\Delta\tau_i$-term in the exponent which is needed to preserve exact normalization condition for the arbitrary x and μ. The second one is the numerically important difference that in our mMRK approach the rapidity-ordering condition is imposed both on quarks and gluons, while in KMR approach it is imposed only on gluons.

To illustrate differences between relevant unPDFs, obtained in the KMR [23,24] model and in our modified model with exact normalization [29], at the different x we plot ratios for integrated over transverse momentum unPDFs to relevant collinear PDFs for the gluon and the valence u-quark as a function of x at the different values of hard scale μ in Fig. 1, left and right panels, correspondingly. We have found sufficient difference for both PDFs.

In contrast to most of the studies in the k_T-factorization, the gauge-invariant matrix elements with off-shell initial-state partons (Reggeized quarks and gluons) from Lipatov's EFT [30,31] allows one to study arbitrary processes involving non-Abelian structure of QCD without violation of Slavnov-Taylor identities due to the nonzero virtuality of initial-state partons. This approach, together with KMR-type unPDFs gives stable and consistent results in a wide range of phenomenological applications, which include the description of the angular correlations of dijets [32], charmed [38,39] and bottom-flavored [33,40] mesons, charmonia [41,42] as well as some other examples.

III. DETAILS OF NUMERICAL CALCULATIONS

The first step of calculations in the PRA is a generation of amplitudes of relevant off-shell partonic processes by Feynman rules of Lipatov EFT. It can be done using a model file ReggeQCD [43] for the FeynArts tool [44]. There are 13 Feynman diagrams for the LO process

TABLE I. The PRA predictions for $p + p \to \gamma\gamma\gamma + X$ total cross section at the $\sqrt{s} = 8$ TeV for the different choice of factorization/renormalization scale ($\mu = \mu_F = \mu_R$). The errors indicate upper and lower limits on the cross sections due to scale uncertainty.

Hard scale, μ	$\sigma_{\rm LO}(Q\bar{Q} \to 3\gamma)$ [fb]	$\sigma(QR \to 3\gamma q)$ [fb]	$\sigma_{\rm NLO}$ [fb]
$M_{3\gamma}$	$37.20^{+9.25}_{-7.98}$	$36.94^{-6.14}_{+5.91}$	$73.14^{+4.13}_{-1.07}$
$E_{T,\Sigma}$	$36.35^{+8.38}_{-9.77}$	$39.26^{-6.29}_{+6.00}$	$75.62^{+3.59}_{-2.39}$

$$Q\bar{Q} \to \gamma\gamma\gamma. \tag{7}$$

The number of EFT diagrams for the NLO in α_S involved in our study for process

$$QR \to q\gamma\gamma\gamma \tag{8}$$

is getting too large for analytical calculation. The full gauge-invariant set of Feynman diagrams contains 40 ones. To proceed next step, we should analytically calculate squared off-shell amplitudes and perform a numerical calculation using factorization formula (1) with modified unPDFs (5). At present, we can do it with the required numerical accuracy only for $2 \to 2$ and $2 \to 3$ off-shell parton processes. To calculate contributions from $2 \to 4$ processes with initial Reggeized partons we apply parton-level generator KaTie [45].

A few years ago, a new approach to deriving gauge-invariant scattering amplitudes with off-shell initial-state partons for high-energy scattering, using the spinor-helicity techniques and BCFW-like recursion relations for such amplitudes have been introduced in the Refs. [46,47]. Sometime later the MC parton-level event generator KaTie [45] has been developed to provide calculations for hadron scattering processes that can deal with partonic initial-state momenta with an explicit transverse momentum dependence causing them to be spacelike. The formalism [46,47] for numerical generation of off-shell amplitudes is equivalent to the results of Lipatov's EFT at the tree level [32,33,48]. We should note here, for the generalization of the formalism to full NLO level [34,35], the use of explicit Feynman rules and the structure of EFT is more convenient.

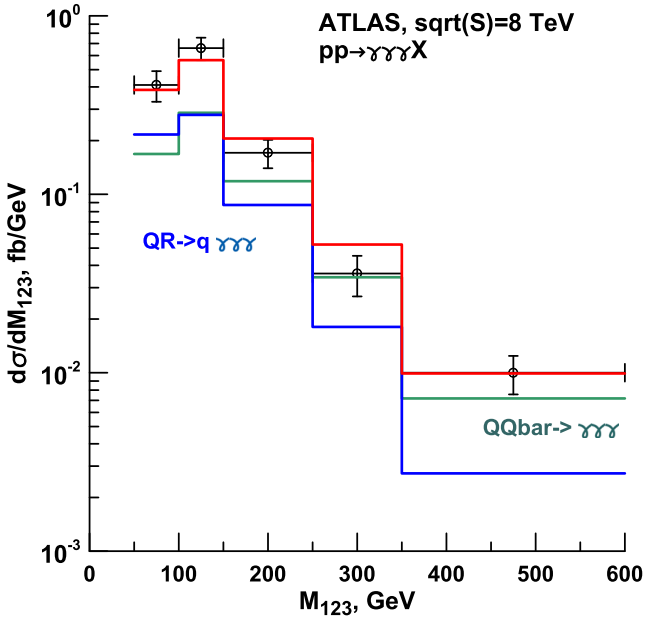

FIG. 2. The differential cross section for the production of three isolated photons as a function of an invariant mass of three-photon system $M_{3\gamma} = M_{123}$. The green histogram corresponds LO contribution from $Q\bar{Q} \to \gamma\gamma\gamma$ subprocess. The blue histogram corresponds NLO contribution from $QR \to q\gamma\gamma\gamma$ subprocess. The red histogram is their sum.

Taking in mind above mentioned discussion, the cross-check calculations of the LO contribution of the subprocess (7) make up both with the KaTie MC generator and using the direct integration of squared amplitudes obtained with the help of Feynman rules of the Lipatov EFT. We perform all final calculations using MC event generator KaTie [45].

We neglect the NLO contribution to the quark-antiquark annihilation channel from subprocesses with the additional final gluon

$$Q\bar{Q} \to g\gamma\gamma\gamma, \tag{9}$$

which should be negligibly small in comparison with main others as in the similar case of the NLO CPM calculations. First of all, because the relevant values of involving longitudinal parton momenta are very small ($x < 10^{-2}$) at the energy range of the LHC, and the gluon density is much larger than the quark (antiquark) ones. In such a way,

TABLE II. Predictions for the $p + p \to \gamma\gamma\gamma + X$ total cross section at the different center-of-mass energies, $\sqrt{s}$. Hard scale is taken as $\mu = M_{3\gamma}$. The numerical error of the total cross section calculation is equal to 0.1%.

$\sqrt{s}$ [TeV]	$\sigma_{\rm LO}(Q\bar{Q} \to 3\gamma)$ [fb]	$\sigma(QR \to 3\gamma q)$ [fb]	$\sigma_{\rm NLO}$ [fb]	$\sigma^{\rm CPM}_{\rm NNLO}$ [12]
8	$37.20^{+9.25}_{-7.98}$	$36.94^{-6.14}_{+5.91}$	$73.14^{+4.13}_{-1.07}$	$67.42^{+7.41}_{-5.73}$
13	$61.64^{+16.88}_{-15.63}$	$72.87^{-9.72}_{+10.78}$	$134.51^{+6.10}_{-3.91}$	$114^{+13.64}_{-10.54}$
27	$132.03^{+40.52}_{-35.50}$	$192.96^{-24.61}_{+19.07}$	$324.99^{+15.91}_{-16.43}$	$245.91^{+32.46}_{-24.34}$

we avoid difficulties in a calculation of the process (9), which follow from an infrared divergence, which should be regularized by a contribution from loop correction to the LO process (7) and from double counting between LO (7) and NLO (9) diagrams with emission of an additional gluon. The technique of NLO calculations is still under development in the PRA, see discussions in Refs. [34–36].

The next important issue is that a calculation for the process (8) does not contain soft and collinear singularities in the PRA, after taking into consideration the isolation-cone conditions for the produced photons and partons.

The important property of the PRA is in rapidity ordering between the emissions from PDFs and the emission during the hard scattering of the involved partons. The possible source of the double counting originates from additional emissions present in the unPDFs in LO contribution (7) and from the real emission of quark in the process (8), when the final quark is produced with large rapidity gap between the three-photon cluster. Because the parent gluon is Reggeized in the subprocess (8), the final quark must have a large rapidity gap between the three-photon system as well as between the proton remnant. In such a way, the subtracted term, which should be used to resolve double-counting, corresponds the process with additional Reggeized-parton exchange in the t-channel and it should be negligibly small. The last conclusion may be clarified by numerical calculation of the rapidity distribution for final quark in the process (8), as it has been done recently in the Ref. [22]. For the enough large a module of quark rapidity, to interpret such emission as emission included in the unPDF, cross section of the process (8) becomes very small.

In the Refs. [49,50], another approach to consistent treatment of NLO-correction at the tree-level was proposed in the k_T-factorization approach. Authors suggested that all additional partons in the hard process should have transverse momentum $p_T > p_{TM}$, where $p_{TM} \sim \mu_F$ is the matching point. The additional partons with small $p_T < p_{TM}$ are considered as involved in the unPDFs. In such a way, we can exclude the double-counting between emissions implicity present in the unPDFs in LO matrix elements

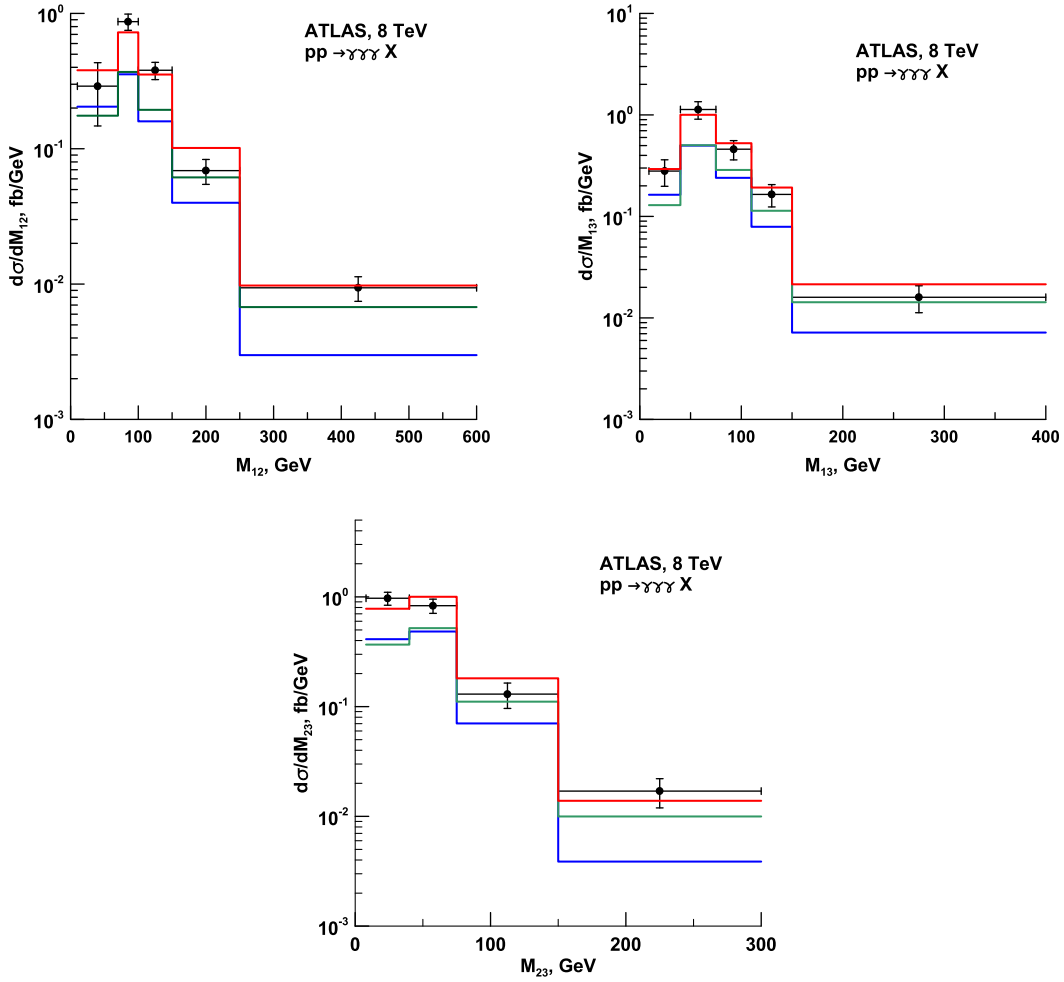

FIG. 3. The differential cross sections for the production of three isolated photons as a function of invariant mass of the photon pairs M_{12}, M_{13}, and M_{23}. The green histogram corresponds the LO contribution from $Q\bar{Q} \to \gamma\gamma\gamma$ subprocess. The blue histogram corresponds the NLO contribution from $QR \to q\gamma\gamma\gamma$ subprocess. The red histogram is their sum.

and emissions are present in the NLO matrix elements. This phenomenological scheme was used in the Ref. [49] for the description of charm production in the noncomplete NLO and NNLO approximations, and in the Ref. [50] for the description of the two-jet correlations in the multijet production processes. We should note here, that such a scheme contradicts the construction of the unPDFs in the KMR model as well as multi-Regge factorization of QCD amplitudes which leads us to Lipatov effective action for Reggeized partons. In both cases, the basic point of consideration is the rapidity ordering between emissions included in the unPDFs and emissions described by the Reggeized amplitude. In the multi-Regge kinematics, there is no correlation between the transverse momenta of emissions in unPDFs (they have large moduli of rapidities) and emissions in the central cluster of the rapidity.

The last remark concerning the calculation is that the numerical accuracy of total cross section calculations with MC generator KaTie by default is 0.1%.

IV. RESULTS

First of all, we review the setup of ATLAS measurements at the $\sqrt{s} = 8$ TeV [5]:

(i) Photon transverse energies (index 1 corresponds to a leading photon, 2—sub-leading photon, and 3—sub-subleading photon) $E_{T1} > 27\,\text{GeV}$, $E_{T2} > 22$ GeV, $E_{T3} > 15$ GeV.

(ii) For the rapidity (pseudorapidity) of all photons, one has $|\eta_{1,2,3}| < 2.37$, excluding the range $1.37 < |\eta_{1,2,3}| < 1.56$.

(iii) The invariant mass of the three-photon system $M_{123} = M_{3\gamma} > 50$ GeV.

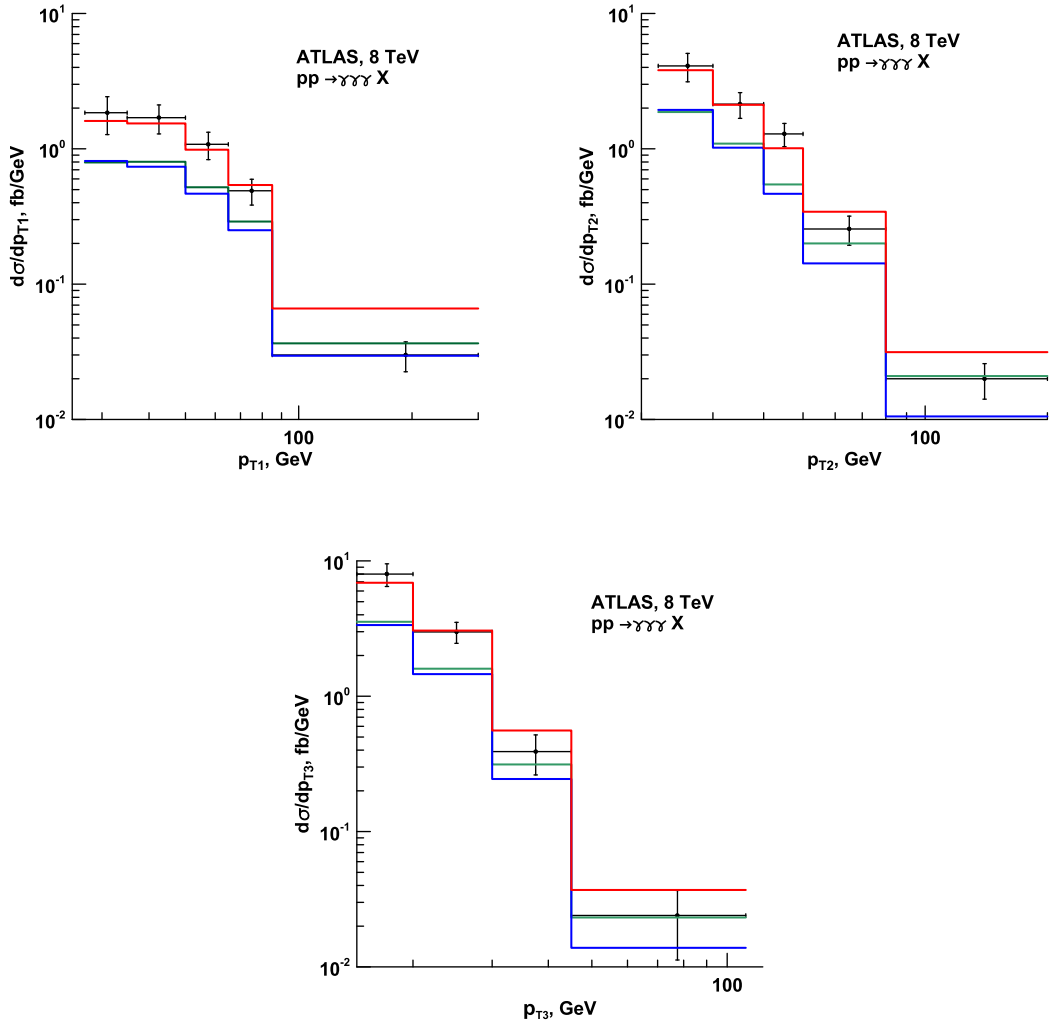

FIG. 4. The differential cross sections for the production of three isolated photons as function of the photon transverse momenta p_{T1} (leading in p_T photons), p_{T2} (next to leading photons) and p_{T3} (next-to-next leading photons). The green histogram corresponds the LO contribution from $Q\bar{Q} \to \gamma\gamma\gamma$ subprocess. The blue histogram corresponds the NLO contribution from $QR \to q\gamma\gamma\gamma$ subprocess. The red histogram is their sum.

(iv) The photon-photon isolation conditions are $\Delta R_{ij} > R_{\gamma\gamma} = 0.45$, where $\Delta R_{ij} = \sqrt{(\eta_i - \eta_j)^2 + (\phi_i - \phi_j)^2}$.

(v) The photon-quark isolation conditions are $\Delta R_{iq} > R_0 = 0.40$.

To take into account a fragmentation contribution, we use the Frixione smooth photon isolation [51]. For any angular difference ΔR_{iq} from each photon, when $\Delta R_{iq} \leq R_0$, it is required

$$E_T^{\rm iso}(\Delta R_{iq}) < E_T^{\rm max} \frac{1 - \cos(\Delta Riq)}{1 - \cos(R_0)},$$

where $E_T^{\rm max} = 10$ GeV, $E_T^{\rm iso} = E_{Tq}$.

We test the dependence of the predicted cross section on a choice of the factorization (μ_F) and renormalization (μ_R) scales, which we take equal to each other, $\mu_F = \mu_R = \mu$. In the Table I we compare predictions obtained with $\mu = M_{3\gamma}$—the invariant mass of the three-photon system and $\mu = E_{T,\Sigma} = E_{T,1\gamma} + E_{T,2\gamma} + E_{T,3\gamma}$—the sum of the transverse momenta (transverse energies) module of photons. Errors indicate upper and lower limits of the cross section obtained due to variation of the hard scale μ by the factors $\xi = 2$ or $\xi = 1/2$ around the central value of the hard scale.

As we see in Table I, where the three-photon production total cross sections are presented, the relative contribution of LO subprocesses grow with the increase of the hard scale μ value and contribution of NLO subprocess oppositely falls, however, the sum changes only a little. Predicted absolute values of cross section are in quite well agreement with the experimental data [5], $\sigma_{\rm exp} = 72.2 \pm 16.7$ fb, as well as with the NNLO CPM results [11,12], taking in mind the level of accuracy, which originated from the scale variation.

At higher energies, $\sqrt{s} = 13$ TeV and $\sqrt{s} = 27$ TeV, the PRA predicts larger cross sections in comparing with the NNLO CPM calculations, see Table II. We estimate

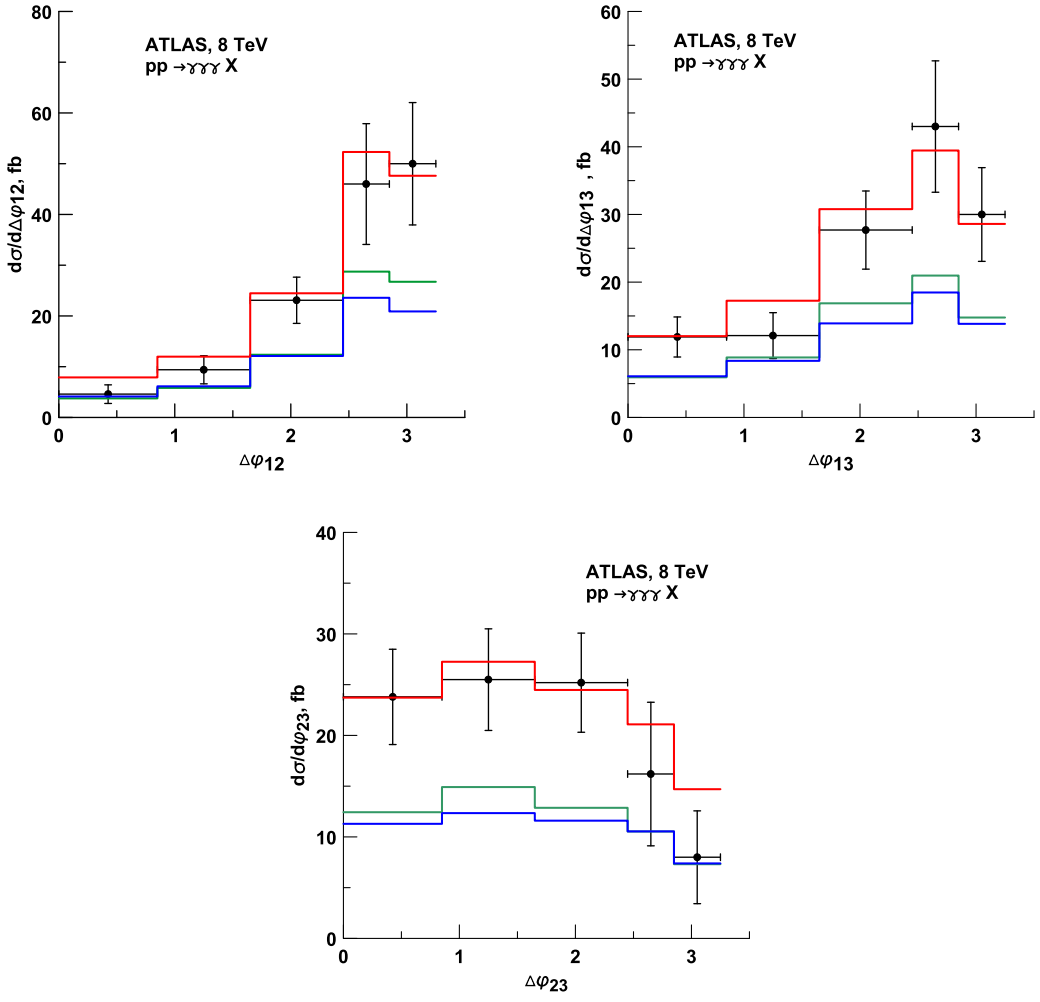

FIG. 5. The differential cross sections for the production of three isolated photons as a function of azimuthal angle difference of the photon pairs, $|\Delta\phi_{12}|$, $|\Delta\phi_{13}|$ and $\Delta\phi_{23}$. The green histogram corresponds the LO contribution from $Q\bar{Q} \to \gamma\gamma\gamma$ subprocess. The blue histogram corresponds the NLO contribution from $QR \to q\gamma\gamma\gamma$ subprocess. The red histogram is their sum.

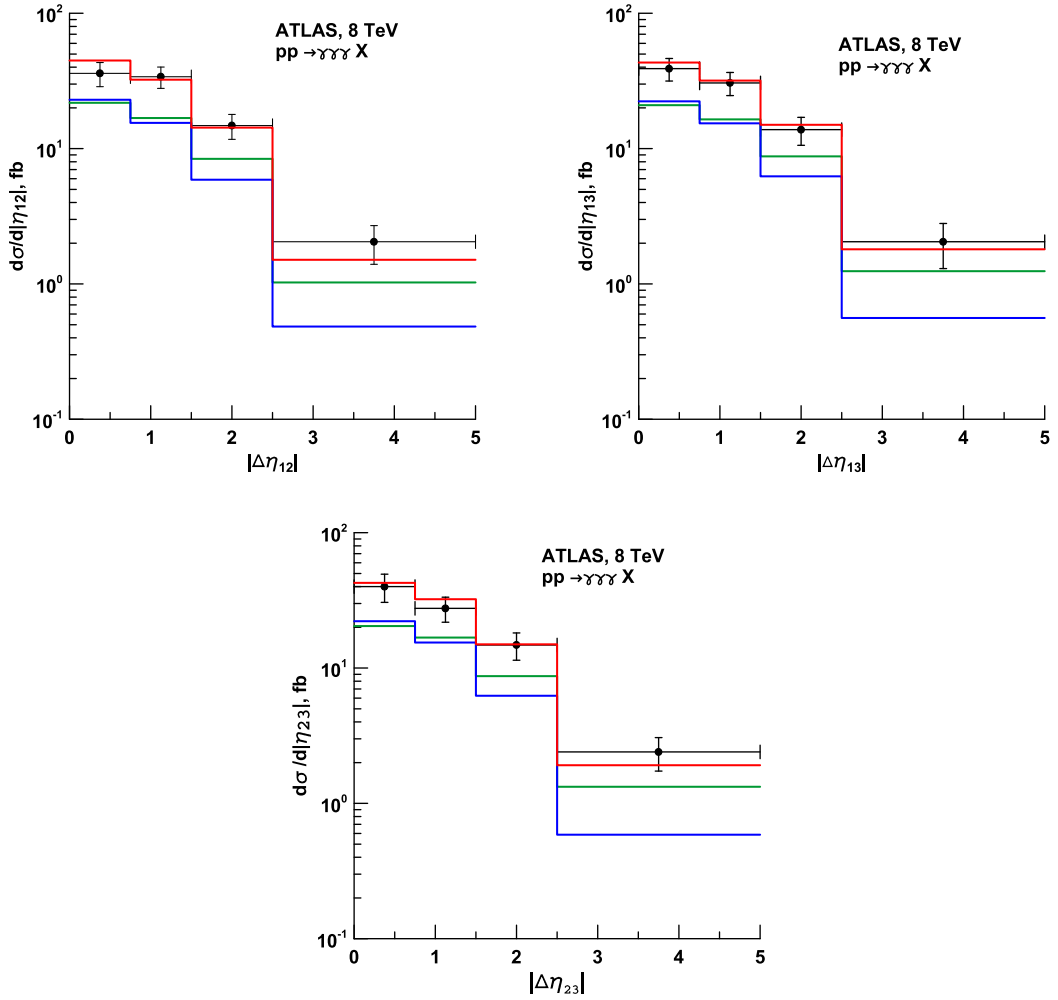

FIG. 6. The differential cross sections for the production of three isolated photons as a function of pseudorapidity differences of the photon pairs $|\Delta\eta_{12}|$, $|\Delta\eta_{13}|$ and $|\Delta\eta_{23}|$. The green histogram corresponds the LO contribution from $Q\bar{Q} \to \gamma\gamma\gamma$ subprocess. The blue histogram corresponds the NLO contribution from $QR \to q\gamma\gamma\gamma$ subprocess. The red histogram is their sum.

excess approximately in 15% and 30%, correspondingly. In the PRA we obtain also a strong decreasing of scale uncertainty in the NLO approximation instead of the LO one as it is estimated from the general properties of the perturbative QCD. One has LO scale uncertainty is about 25%–30%, but at NLO level of calculation, it is only 4%-5% at different energies. Let us note that in the NNLO CPM calculation of three-photon production cross section [11,12] such uncertainty is still about 10%.

The differential spectra, which demonstrate different kinematics correlations between final photons, are shown in Figs. 2–6. The central choice of the hard scale in these calculations is taken as the invariant mass of the three-photon system, $\mu = M_{3\gamma}$. There are no kinematics regions in invariant masses, pseudorapidities, azimuthal angles, or transverse momenta where one of the studied here contributions can be considered a dominant one. To describe the data, the both should be taken into account. The NLO contribution in α_s (8) is enhanced evidently because it is proportional to a quark-gluon luminosity instead of a quark-antiquark luminosity in the case of the LO production (7) in proton-proton collision.

V. CONCLUSIONS

We obtain a quite satisfactory description for cross section and spectra for the three-photon production in the LO PRA with a matching of the real NLO correction from the partonic subprocess (8) at the $\sqrt{s} = 8$ TeV. We demonstrate the applicability of the new KMR-type quark and gluon unPDFs with exact normalization to use in high-energy factorization calculations. It has been shown that, as in our previous studies of hard processes in the PRA, obtained results in the LO approximation coincide with full

NLO predictions of the CPM and, respectively, the NLO calculations in the PRA roughly reproduce NNLO predictions of the CPM. However, at higher energies (13 and 27 TeV) the PRA predicts a larger cross sections, up to ∼15% and ∼30%, with respect to predictions of the NNLO CPM. The last fact can be used for a discrimination between the high-energy factorization and the collinear factorization for hard processes at high energies.

ACKNOWLEDGMENTS

We are grateful to A. van Hameren for helpful communication on MC generator KaTie, M. Nefedov and A. Shipilova for useful physics discussions. The work has been supported in parts by the Ministry of Science and Higher Education of Russia via State assignment to educational and research institutions under Project No. FSSS-2020-0014.

[1] T. Aaltonen *et al.* (CDF Collaboration), Measurement of the cross section for prompt isolated diphoton production in $p\bar{p}$ collisions at $\sqrt{s} = 1.96$ TeV, Phys. Rev. D **84**, 052006 (2011).
[2] T. Aaltonen *et al.* (CDF Collaboration), Measurement of the Cross Section for Prompt Isolated Diphoton Production Using the Full CDF Run II Data Sample, Phys. Rev. Lett. **110**, 101801 (2013).
[3] G. Aad *et al.* (ATLAS Collaboration), Measurement of isolated-photon pair production in pp collisions at $\sqrt{s} =$ 7 TeV with the ATLAS detector, J. High Energy Phys. 01 (2013) 086.
[4] S. Chatrchyan *et al.* (CMS Collaboration), Measurement of differential cross sections for the production of a pair of isolated photons in pp collisions at $\sqrt{s} = 7$ TeV, Eur. Phys. J. C **74**, 3129 (2014).
[5] M. Aaboud *et al.* (ATLAS Collaboration), Measurement of the production cross section of three isolated photons in pp collisions at $\sqrt{s} = 8$ TeV using the ATLAS detector, Phys. Lett. B **781**, 55 (2018).
[6] T. Binoth, J. P. Guillet, E. Pilon, and M. Werlen, A full next-to-leading order study of direct photon pair production in hadronic collisions, Eur. Phys. J. C **16**, 311 (2000).
[7] J. M. Campbell and C. Williams, Triphoton production at hadron colliders, Phys. Rev. D **89**, 113001 (2014).
[8] J. Alwall, R. Frederix, S. Frixione, V. Hirschi, F. Maltoni, O. Mattelaer, H.-S. Shao, T. Stelzer, P. Torrielli, and M. Zaro, The automated computation of tree-level and next-to-leading order differential cross sections, and their matching to parton shower simulations, J. High Energy Phys. 07 (2014) 079.
[9] S. Catani, L. Cieri, D. de Florian, G. Ferrera, and M. Grazzini, Diphoton Production at Hadron Colliders: A Fully-Differential QCD Calculation at NNLO, Phys. Rev. Lett. **108**, 072001 (2012); Erratum, Phys. Rev. Lett. **117**, 089901 (2016).
[10] J. M. Campbell, R. K. Ellis, Y. Li, and C. Williams, Predictions for diphoton production at the LHC through NNLO in QCD, J. High Energy Phys. 07 (2016) 148.
[11] H. A. Chawdhry, M. L. Czakon, A. Mitov, and R. Poncelet, NNLO QCD corrections to three-photon production at the LHC, J. High Energy Phys. 02 (2020) 057.
[12] S. Kallweit, V. Sotnikov, and M. Wiesemann, Triphoton production at hadron colliders in NNLO QCD, Phys. Lett. B **812**, 136013 (2021).
[13] J. Collins, Foundations of perturbative QCD, Cambridge Monogr. Part. Phys., Nucl. Phys., Cosmol. **32**, 1 (2011).
[14] L. N. Lipatov, Reggeization of the vector meson and the vacuum singularity in non-Abelian gauge theories, Yad. Fiz. **23**, 642 (1976) [Sov. J. Nucl. Phys. **23**, 338 (1976)].
[15] E. A. Kuraev, L. N. Lipatov, and V. S. Fadin, Multi—Reggeon processes in the Yang-Mills theory, Zh. Eksp. Teor. Fiz. **71**, 840 (1976) [Sov. Phys. JETP **44**, 443 (1976)].
[16] E. A. Kuraev, L. N. Lipatov, and V. S. Fadin, The Pomeranchuk singularity in non-Abelian gauge theories, Zh. Eksp. Teor. Fiz. **72**, 377 (1977) [Sov. Phys. JETP **45**, 199 (1977)].
[17] I. I. Balitsky and L. N. Lipatov, The Pomeranchuk singularity in quantum chromodynamics, Yad. Fiz. **28**, 1597 (1978) [Sov. J. Nucl. Phys. **28**, 822 (1978)].
[18] B. A. Kniehl, V. A. Saleev, A. V. Shipilova, and E. V. Yatsenko, Single jet and prompt-photon inclusive production with multi-Regge kinematics: From Tevatron to LHC, Phys. Rev. D **84**, 074017 (2011).
[19] M. Nefedov and V. Saleev, Diphoton production at the Tevatron and the LHC in the NLO approximation of the parton Reggeization approach, Phys. Rev. D **92**, 094033 (2015).
[20] A. Karpishkov, V. Saleev, and A. Shipilova, Angular decorrelations in $\gamma + 2jet$ events at high energies in the parton Reggeization approach, Mod. Phys. Lett. A **34**, 1950266 (2019).
[21] V. Saleev, Production of three isolated photons in the high-energy factorization approach, SciPost Phys. Proc. **8**, 167 (2022).
[22] R. K. Valeshabadi, M. Modarres, and S. Rezaie, Three-photon productions within the k_t-factorization at the LHC, Eur. Phys. J. C **81**, 961 (2021).
[23] M. A. Kimber, A. D. Martin, and M. G. Ryskin, Unintegrated parton distributions, Phys. Rev. D **63**, 114027 (2001).
[24] G. Watt, A. D. Martin, and M. G. Ryskin, Unintegrated parton distributions and inclusive jet production at HERA, Eur. Phys. J. C **31**, 73 (2003).
[25] F. Hautmann, H. Jung, A. Lelek, V. Radescu, and R. Zlebcik, Collinear and TMD quark and gluon densities from parton branching solution of QCD evolution equations, J. High Energy Phys. 01 (2018) 070.
[26] A. Bermudez Martinez, P. Connor, H. Jung, A. Lelek, R. Žlebčík, F. Hautmann, and V. Radescu, Collinear and TMD parton densities from fits to precision DIS measurements in

the parton branching method, Phys. Rev. D **99**, 074008 (2019).
[27] J. C. Collins and R. K. Ellis, Heavy quark production in very high-energy hadron collisions, Nucl. Phys. **B360**, 3 (1991).
[28] S. Catani and F. Hautmann, High-energy factorization and small x deep inelastic scattering beyond leading order, Nucl. Phys. **B427**, 475 (1994).
[29] M. A. Nefedov and V. A. Saleev, High-energy factorization for Drell-Yan process in pp and $p\bar{p}$ collisions with new unintegrated PDFs, Phys. Rev. D **102**, 114018 (2020).
[30] L. N. Lipatov, Gauge invariant effective action for high-energy processes in QCD, Nucl. Phys. **B452**, 369 (1995).
[31] L. N. Lipatov and M. I. Vyazovsky, Quasi-multi-Regge processes with a quark exchange in the t channel, Nucl. Phys. **B597**, 399 (2001).
[32] M. A. Nefedov, V. A. Saleev, and A. V. Shipilova, Dijet azimuthal decorrelations at the LHC in the parton Reggeization approach, Phys. Rev. D **87**, 094030 (2013).
[33] A. V. Karpishkov, M. A. Nefedov, and V. A. Saleev, $B\bar{B}$ angular correlations at the LHC in parton Reggeization approach merged with higher-order matrix elements, Phys. Rev. D **96**, 096019 (2017).
[34] M. Nefedov and V. Saleev, On the one-loop calculations with Reggeized quarks, Mod. Phys. Lett. A **32**, 1750207 (2017).
[35] M. A. Nefedov, Towards stability of NLO corrections in high-energy factorization via modified multi-Regge kinematics approximation, J. High Energy Phys. 08 (2020) 055.
[36] M. A. Nefedov, Computing one-loop corrections to effective vertices with two scales in the EFT for multi-Regge processes in QCD, Nucl. Phys. **B946**, 114715 (2019).
[37] E. N. Antonov, L. N. Lipatov, E. A. Kuraev, and I. O. Cherednikov, Feynman rules for effective Regge action, Nucl. Phys. **B721**, 111 (2005).
[38] R. Maciuła, V. A. Saleev, A. V. Shipilova, and A. Szczurek, New mechanisms for double charmed meson production at the LHCb, Phys. Lett. B **758**, 458 (2016).
[39] A. V. Karpishkov, M. A. Nefedov, V. A. Saleev, and A. V. Shipilova, B-meson production in the parton Reggeization Approach at Tevatron and the LHC, Int. J. Mod. Phys. A **30**, 1550023 (2015).
[40] A. Karpishkov, V. Saleev, and A. Shipilova, Large-p_T production of D mesons at the LHCb in the parton Reggeization approach, Phys. Rev. D **94**, 114012 (2016).
[41] V. A. Saleev, M. A. Nefedov, and A. V. Shipilova, Prompt J/psi production in the Regge limit of QCD: From Tevatron to LHC, Phys. Rev. D **85**, 074013 (2012).
[42] Z. G. He, B. A. Kniehl, M. A. Nefedov, and V. A. Saleev, Double Prompt J/ψ Hadroproduction in the Parton Reggeization Approach with High-Energy Resummation, Phys. Rev. Lett. **123**, 162002 (2019).
[43] See Supplemental Material at https://link.aps.org/supplemental/10.1103/PhysRevD.92.094033 to obtain the ReggeQCD model file.
[44] T. Hahn, Generating Feynman diagrams and amplitudes with FeynArts 3, Comput. Phys. Commun. **140**, 418 (2001).
[45] A. van Hameren, KaTie: For parton-level event generation with k_T-dependent initial states, Comput. Phys. Commun. **224**, 371 (2018).
[46] A. van Hameren, P. Kotko, and K. Kutak, Helicity amplitudes for high-energy scattering, J. High Energy Phys. 01 (2013) 078.
[47] A. van Hameren, K. Kutak, and T. Salwa, Scattering amplitudes with off-shell quarks, Phys. Lett. B **727**, 226 (2013).
[48] K. Kutak, R. Maciula, M. Serino, A. Szczurek, and A. van Hameren, Four-jet production in single- and double-parton scattering within high-energy factorization, J. High Energy Phys. 04 (2016) 175.
[49] R. Maciula and A. Szczurek, Consistent treatment of charm production in higher-orders at tree-level within k_T-factorization approach, Phys. Rev. D **100**, 054001 (2019).
[50] M. A. Nefedov and V. A. Saleev, Two-jet correlations in multijet events in the Regge limit of QCD, Phys. Part. Nucl. **51**, 714 (2020).
[51] S. Frixione, Isolated photons in perturbative QCD, Phys. Lett. B **429**, 369 (1998).